

RADIO EMISSION OF RYDBERG ATOMS IN THE UPPER ATMOSPHERE MODIFIED BY HIGH-POWER HF RADIO WAVES

A. V. Troitskii,^{1*} V. L. Frolov,^{1,2} A. V. Vostokov,¹
and I. V. Rakut,¹

UDC 533.9+550.348

We report on the results of studying the radio emission of the Rydberg states of atoms and molecules in the Earth's upper atmosphere at ionospheric altitudes when the ionosphere is modified by high-power HF radio waves radiated by the Sura heating facility. Radio emission from the upper atmosphere, caused by the emission of highly excited Rydberg atoms and molecules with the principal quantum number $n = 163$ – 169 and $n = 225$ (decimeter wavelength range) and two spectral features that coincide with the frequencies of transitions between Rydberg states $m = 169 \rightarrow n = 168$ with the transition frequency $\nu_n = 1375.35$ MHz and $m = 166 \rightarrow n = 165$ with $\nu_n = 1451.5$ MHz were detected. Characteristic altitudes of the Rydberg radiation generation region were 150–250 km. The radio emission intensity corresponds to 10–45 K, which is comparable with the intensity of the radio emission generated during solar flares.

1. INTRODUCTION

The ionosphere, like any heated body, emits electromagnetic energy in a wide wavelength range of radio waves. This thermal radiation is of fluctuation nature and is generated by the chaotic motion of charged particles with the Maxwell distribution of their velocities. The intensity of thermal radiation of the ionosphere in the scale of radio brightness temperatures is several degrees and a few tenths of a degree in the meter and decimeter wavelength ranges, respectively [1]. In this case, the electron temperature of the ionosphere is 1000–1500 K. When the ionospheric F_2 region is affected by high-power HF O-mode radio waves, considerable heating of the plasma electrons to temperatures of up to 3000–4500 K occurs near their reflection height. Accordingly, the intensity of thermal radiation is enhanced in the decimeter and meter wavelength ranges.

In [2, 3], high-power sporadic microwave radiation, the intensity of which corresponded to tens of degrees of brightness temperature, was detected in the ionosphere in a wide range of centimeter and decimeter waves. It was found that this radiation correlates with a solar activity burst and related geomagnetic disturbances [4, 5]. Only 25 years later, the nature of this phenomenon was explained in [6] on the basis of the Rydberg mechanism of emission of neutral atoms and molecules at ionospheric altitudes. This mechanism includes transitions of electrons between highly excited (the main quantum number $n > 10$) Rydberg levels of neutral atoms and molecules of the ionosphere, which are excited as they collide with a flow of high-energy solar particles. Note that the emission radio lines corresponding to transitions between Rydberg states up to $n \approx 300$ were observed in the galactic regions of ionized hydrogen H II and in planetary nebulas [7]. A similar mechanism, but due to accelerated electrons of the ionospheric plasma heated by high-power HF

* avTroitskii@yandex.ru

¹ N. I. Lobachevsky State University of Nizhny Novgorod, Nizhny Novgorod; ² Kazan (Volga) Federal University, Kazan, Russia. Translated from *Izvestiya Vysshikh Uchebnykh Zavedenii, Radiofizika*, Vol. 62, No. 10, pp. 759–768, October 2019. Original article submitted May 17, 2019; accepted October 30, 2019.

radio waves, was used for interpretation of artificial radiation of the ionosphere in the decimeter wavelength range [8]. Collective Rydberg states in the upper atmosphere of the Earth were considered in detail in [9].

After the detection of HF-stimulated precipitation of high-energy electrons from the Earth's radiation belts it became topical to detect the possibility of excitation of Rydberg states of atoms and molecules at ionospheric altitudes during operation of high-power radio emission sources.

The proposed work discusses the results of recent experimental studies of the Rydberg radiation of the ionospheric neutral component stimulated by high-power HF radiation from the Sura facility, which is located at mid-latitudes 130 km east of the city of Nizhny Novgorod.

2. RYDBERG ATOMS IN THE IONOSPHERIC PLASMA

Rydberg states are highly excited states of the atoms and molecules which are located near the ionization threshold and are characterized by an infinite sequence of energy levels in the near-threshold range of energies. Rydberg atoms and molecules have a single highly excited, weakly coupled electron. With extremely strong excitation, an atom (molecule) can be considered as a macroscopic object since at $n = 1000$ its size, determined by the radius of the electron orbit, is $r_n \approx 10^{-8}n^2 \approx 10^{-2}$ cm. Therefore, a Rydberg atom (molecule) can be represented as a positively charged ion bone and a Rydberg electron. For many problems, the ion bone can be regarded as a point positive charge, and a hydrogen-like atom can be considered as the model of a Rydberg atom. In such a model, the energies of the Rydberg states of an isolated atom, which are reckoned from the ionization energy, are determined by the Rydberg formula

$$E_n = R(1 - m_e/M)(n - \delta)^{-2}, \quad (1)$$

where $R = 13.6058$ eV is the energy Rydberg constant, m_e is the electron mass, M is the nuclear mass, and δ is a quantum defect of the nuclear charge, the contribution of which is negligibly small for high n .

TABLE 1. Main parameters of the Rydberg states of atoms (approximate values) compared with the main state ($n = 2$).

	Principal quantum number n	2	1000
1	Electron coupling energy in atom (ionization potential), eV	5	10^{-5}
2	Size of atom (radius of electron orbit), cm	10^{-8}	10^{-2}
3	Orbital revolution period of electron, s	10^{-15}	10^{-6}
4	Natural lifetime, s	10^{-8}	10
5	Frequency of transitions between the neighboring states, MHz	10^9	1

Rydberg states are metastable: the lifetime of a Rydberg atom for $n = 1000$ is $\tau_n \approx 10^{-8} n^3 \approx 10$ s. The frequency of transitions between the Rydberg levels $m \rightarrow n$ is determined by the expression

$$\nu = R_\nu(1 - m_e/M)(1/n^2 - 1/m^2), \quad (2)$$

where $R_\nu = 3.289842 \cdot 10^{15}$ Hz is the Rydberg spectroscopic constant. It follows from Eq. (2) that transitions $(n + 1) \rightarrow n$ between the neighboring states correspond to the radio-wave frequencies $\nu_n \approx 2R_\nu n^{-3}$, which lie in the submillimeter and millimeter ranges at $n \approx 25$ –60, in the centimeter range at $n \approx 60$ –130, and in the decimeter range at $n \approx 130$ –280. It should specially be noted that the distance $\Delta\nu_n$ between the neighboring Rydberg lines is $\Delta\nu_{103} \approx 170$ MHz in the centimeter range, $\Delta\nu_{221} \approx 8$ MHz in the decimeter range, and the radiation spectrum becomes almost continuous in the meter range at $n > 300$ with allowance for different factors of the line broadening (collisions, Doppler effect, Zeeman effect, etc.).

The main characteristics of the atoms which are in the first excited state $n = 2$ and Rydberg atoms with $n = 1000$ are given in Table 1 for comparison.

We note that the density of neutral atoms and molecules (N_2 , O_2 , and O) in the ionospheric F_2 layer is $N_a \approx 10^9$ cm $^{-3}$, which corresponds to a distance of about 10^{-3} cm between them. This value is comparable with the sizes of Rydberg atoms and molecules at $n > 300$. In this case, their orbits start to touch each

other, which leads to a significant enhancement of the collisional and radiation interactions between them, which play a great role in the physical and chemical processes occurring in the Earth's atmosphere. In addition, at ionospheric altitudes, the lifetime τ of the Rydberg states of atoms and molecules is determined by the frequency of their collisions with electrons $\nu_E \sim 500 \text{ s}^{-1}$, which corresponds to $\tau \sim 2 \cdot 10^{-3} \text{ s}$.

The main natural mechanisms of the formation of Rydberg states at ionospheric altitudes include the processes of photo excitation during absorption of solar hard ultraviolet radiation and excitation that occurs when energetic electrons of the solar flares and electrons precipitating from the Earth's radiation belts in strong geomagnetic disturbances collide with atoms and molecules of the ionosphere, as well as dissociative excitation. Since the ionization potential of the main atoms and molecules N_2 , O_2 and O of the atmosphere at ionospheric altitudes is 15.5, 12.2, and 13.62 eV, respectively, which is much less than the energy of indicated processes, the latter are quite able to excite atoms and molecules up to pre-ionization levels and even ionize them. Then, in the process of transition of Rydberg atoms and molecules to the lower states, a wide spectrum of electromagnetic waves from radio-frequency to ultraviolet radiation is emitted. According to experimental data [2–5], the intensity of this radiation in the decimeter wavelength range is comparable to or even exceeds typical levels of solar radiation bursts during solar flares. Microwave components of Rydberg radiation reach the Earth's troposphere almost without loss and can lead to a change in the physical characteristics of the surface atmosphere (see, e. g., [10–12]).

3. MEASUREMENT PROCEDURE AND THE RESULTS

This paper considers an artificial mechanism for the formation of Rydberg states at the Earth ionospheric altitudes, which is due to the effect of high-power HF radio waves on the plasma of the ionospheric F_2 layer (altitudes 200–300 km). The mechanism is based on the ionospheric plasma modification by high-power O-mode radio waves with different plasma instabilities developing near their reflection heights. These instabilities lead to the excitation of intense plasma turbulence (plasma waves, artificial ionospheric irregularities, etc.), which finally leads to a strong plasma heating where the electron temperature T_e in the plasma can increase by a factor of 2–3 [13–16]. Such an increase in T_e , as well as the acceleration of background electrons in the regions with intense high-frequency plasma turbulence leads to the appearance of electrons with energies of up to 5–30 eV [14, 15]. These “hot” electrons have an energy higher than the ionization potential of N_2 , O_2 and O , and they can, by colliding with these molecules, convert them into a highly excited Rydberg state or cause additional artificial ionization of the atmosphere. Recent research has shown [17] that high-energy electrons $E \approx 100 \text{ keV}$ can appear at ionospheric altitudes due to their precipitation from the Earth's radiation belt stimulated by heating of the F_2 region by high-power radio waves. These electrons, as in the case of solar radiation, can also convert them into highly excited Rydberg states as a result of their multiple collisions with atoms and molecules of the atmosphere. At the next step, there occur transitions into lower energy states, with radiation of a wide spectrum of electromagnetic waves, due to collisions of Rydberg atoms with low-energy electrons and neutral atoms, as well as spontaneously.

Characteristics of the microwave radiation generated at ionospheric altitudes when the ionosphere is modified by high-power HF radio waves emitted by Sura, a midlatitude heating facility (Radiophysical Research Institute of the Nizhny Novgorod State University), were studied in 2014–2018. The heater radiated O-mode waves in the frequency range 4.3–6.8 MHz, usually in the [10–15 min radiation — 10–15-min pause] regime with an effective power of 80–180 MW, which increased with increasing frequency f_{PW} of the pump wave. The antenna of the Sura facility is $300 \times 300 \text{ m}$, and its radiation pattern is about 14° at pump-wave frequencies of about 5 MHz. As a rule, a beam of radio waves was radiated at an angle of 12° southward of the vertical line (towards the magnetic zenith region) to increase the ionosphere modification efficiency due to the magnetic zenith effect [14–16]. It should be noted that all the measurements considered in this paper were performed in quiet or very quiet geomagnetic conditions, when the total geomagnetic activity index ΣK_p did not exceed 20, and not only the measurement days, but also a few days prior to them were quiet.

The intensity of the atmospheric microwave radiation was measured using spectral radiometric receivers of modulation type (radiometers) of the decimeter wavelength range at frequencies $f_1 = 1\text{--}2 \text{ GHz}$

TABLE 2. Technical characteristics of the radiometric system.

	Characteristic of receiver	Radiometer, $\lambda \sim 20$ cm	Radiometer, $\lambda \sim 52$ cm
1	Reception frequency, MHz	1350–1500	574
2	Decay outside the reception band, dB	45	35
3	Number of channels	10	1
4	Passband of the channel, MHz	15	5
5	Interval between channels, MHz	15	—
6	Fluctuation sensitivity, K	0.20	0.15
7	Modulation frequency, kHz	1	1
8	Signal integration time, s	1	1
9	Beamwidth of the receiving antenna, deg	14	15

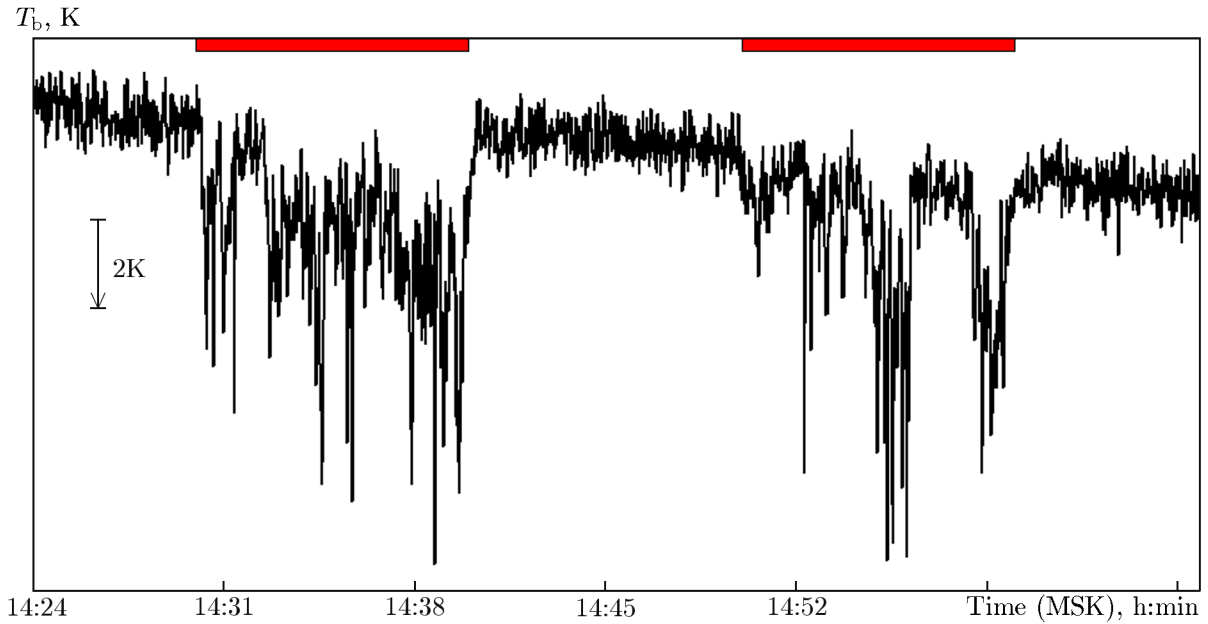


Fig. 1. Atmospheric radiation intensity on September 8, 2014 in the spectral channel band $f = (1450 \pm 8)$ MHz. The brightness temperature increase in Figs. 1–3 corresponds to the downward direction.

and $f_2 = 574$ MHz. Technical characteristics of the radiometric system are given in Table 2. The system was located on the territory of the Sura facility. Radio emission was received using horn-type and parabolic antennas. Spatial orientation of the antenna patterns of the radiometers and the Sura facility coincided. The received radiation was calibrated in the brightness temperature scale with two radiation sources located in the far-field area of the antennas, namely, the sky (zenith brightness temperature $T_b \approx 3$ K) and the Earth’s surface with vegetation ($T_b \approx T_0$, where T_0 is the surface air temperature).

Figures 1 and 2 show examples of recording of the atmospheric radiation (in the brightness temperature scale) in the band of the spectral channel $f_1 = (1450 \pm 8)$ MHz, which corresponds to the frequency $\nu_n = 1451.5$ MHz of a transition between Rydberg states $m = 166 \rightarrow n = 165$. The frequency of the high-power pump radio wave was $f_{PW} = 4300$ kHz for the case in Fig. 1 and $f_{PW} = 5828$ kHz for Fig. 2; in both cases, the heater was operated in the [10-min radiation—10-min pause] regime. Hereafter, the Sura operation time is marked by red rectangles on the time axis. Vertical segment with an arrow on the left in the figures shows the variation scale of the brightness temperature and the direction of its increase. In the first case (Fig. 1), the measurements were performed on September 8, 2014 in the afternoon. The

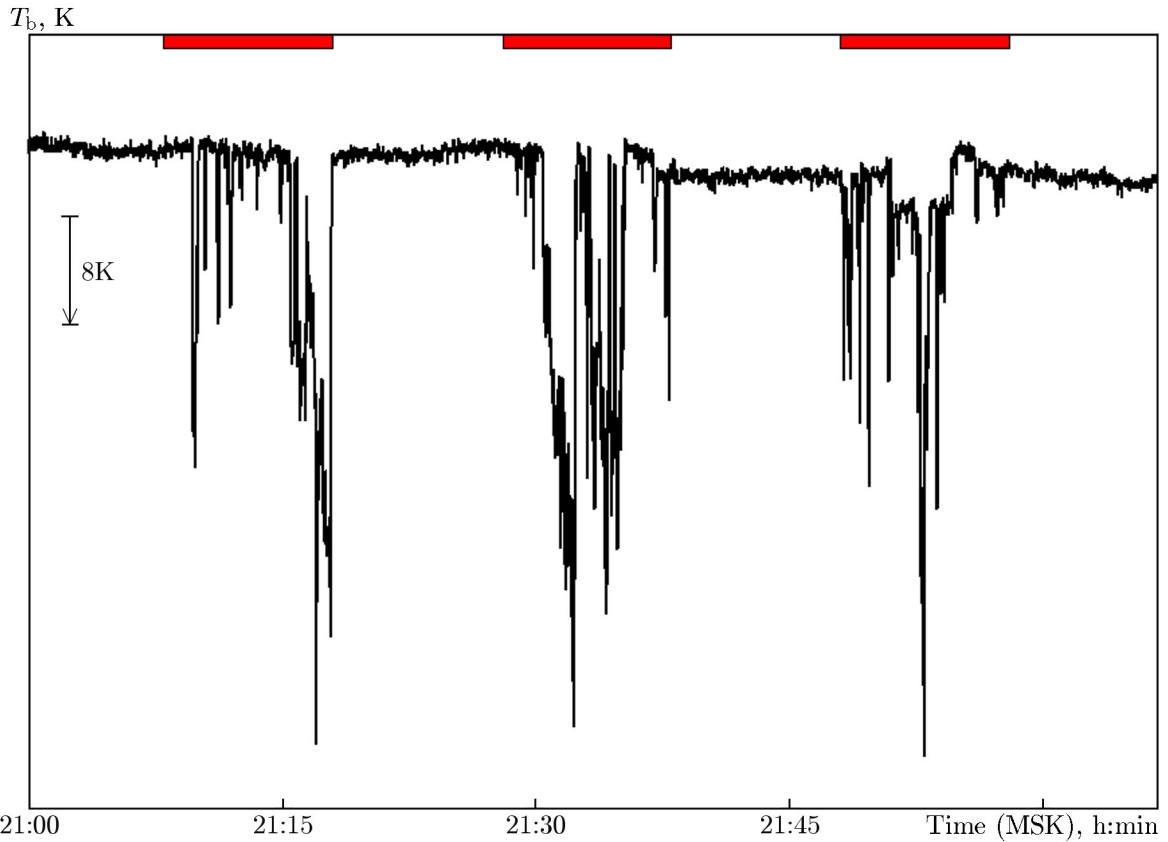


Fig. 2. Atmospheric radiation intensity on March 28, 2014 in the spectral channel band $f = (1450 \pm 8)$ MHz.

recorded peak intensity of Rydberg radiation with $\Delta T_b \approx 9$ K was minimum among all the experiments. In the second case, the experiment was performed on March 28, 2014 late in the evening. In this case, the maximum peak intensity of Rydberg radiation with $\Delta T_b \approx 43$ K was observed.

Figure 3 shows a typical record of the atmospheric radiation intensity measurement in the spectral channel band $f_2 = (574 \pm 3)$ MHz, which corresponds to the frequency $\nu_n = 573.81$ MHz of a transition between Rydberg states $m = 226 \rightarrow n = 225$. The pump wave was radiated at the frequency $f_{PW} = 4300$ kHz, and the heater was operated in the [14-min radiation (30 s on and 30 s off)—16-min pause] regime. It can be seen that the largest microwave radiation intensity was often recorded at the beginning of a 30-s pump pulse, which is a consequence of the overshoot effect that is usually observed when artificial ionospheric turbulence develops [16].

A total of 11 cycles of the ionosphere modification by high-power HF radiation from the Sura facility have been performed in the research period. The results of radiometric measurements of the radiation intensity of Rydberg atoms and molecules of the upper atmosphere are given in Table 3. Rydberg radiation of atoms and molecules of the upper atmosphere in the decimeter wavelength range with the peak intensity corresponding to $\Delta T_b \approx 10$ –26 K in the morning and in the afternoon and to $\Delta T_b \approx 30$ –43 K in the late evening and nighttime hours have been recorded in 7 sessions. These values are in good agreement with the results of measuring the natural sporadic ionospheric radiation intensity during solar flares, which were obtained in [3, 4], and exceed by almost 20–30 times the results of measuring the intensity of artificial ionospheric radiation intensity in the decimeter wavelength range, which was recorded in [8].

The discrepancy with the results of [8] can be determined by the following factors. The measurement scheme in [8] was significantly different from that used in this paper. In our case, the spatial orientation of the antenna patterns of the radiometers and the Sura facility were completely the same. Therefore, the height of the entire region of highly excited Rydberg atoms and molecules automatically fell into the

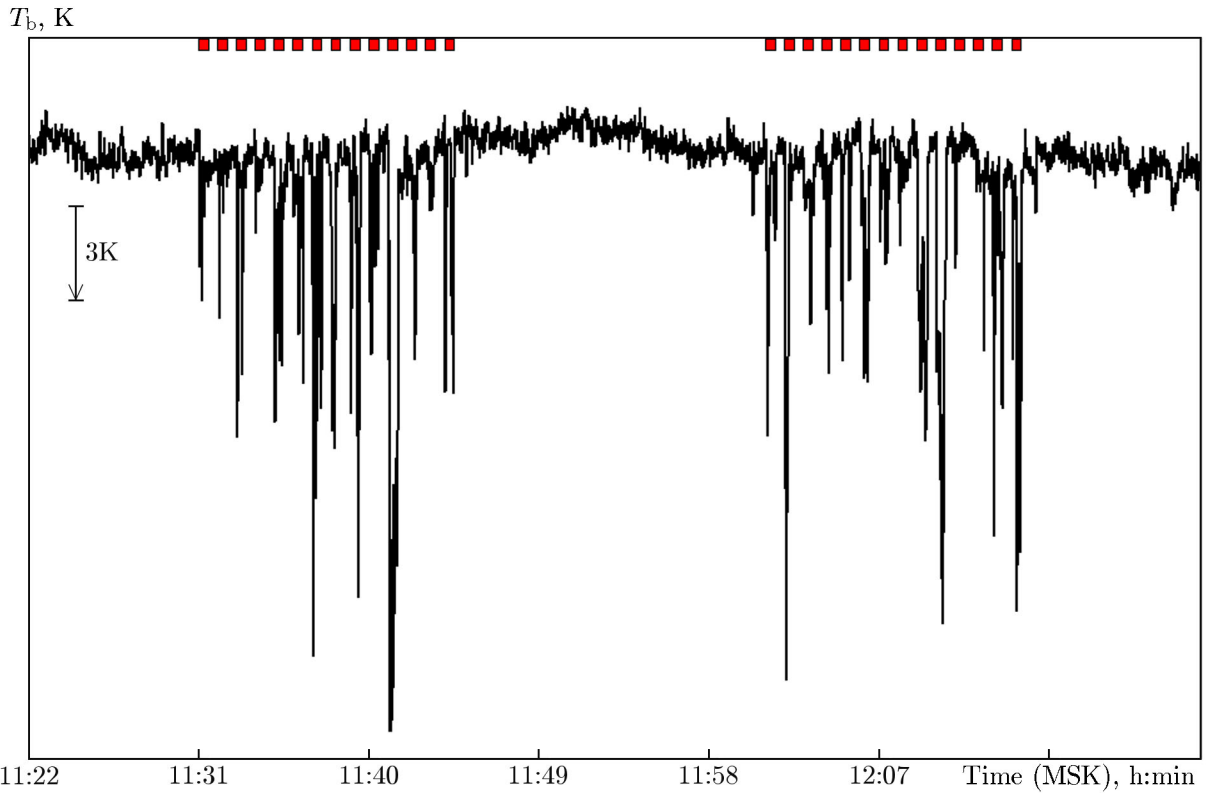


Fig. 3. Atmospheric radiation intensity on August 29, 2018 in the spectral channel band $f = (574 \pm 3)$ MHz.

TABLE 3. Results of measuring the atmospheric radio emission at frequencies $f_1 = (1450 \pm 8)$ MHz (lines 1–5) and $f_2 = (574 \pm 3)$ MHz (lines 6 and 7).

	Date and time	f_{PW} , kHz (f_{0F_2} , MHz); operation mode	Pump wave reflection height h_{ref} , km	Radiation intensity (peak) ΔT_b , K
1	March 27, 2014 21:21–22:11	5828 (7.2 \rightarrow 6.4); [+9 min, -1 min]	240 \rightarrow 270	30
2	March 28, 2014 20:28–22:23	5828 (8.4 \rightarrow 6.5); [± 10 min]	220 \rightarrow 255	43
3	March 29, 2014 00:50–01:10	4300 (5.6); [carrier frequency]	260	38
4	September 8, 2014 14:10–15:20	4300 (-); [± 10 min]	155 \rightarrow 185	9
5	April 2, 2015 17:53–20:33	6720 (8.2 \rightarrow 6.9); [+10 min, -5 min]	220 \rightarrow 285	23
6	August 29, 2018 10:01–12:50	4300 (4.5); [14 min \times (± 30 s), -16 min]	195	20
7	August 30, 2018 09:30–12:00	4300 (4.9); [+14 min, -16 min]	175	26

reception pattern of the radiometers. In [8], the radiometer was at a distance of approximately 110 km west of the heater and the elevation angle of the region of highly excited atoms and molecules was *a priori* unknown. Hence, the location area may not coincide with the area of the most intense generation of Rydberg radiation. It cannot be excluded that the increased radiation intensity in [8] was due to the thermal radiation of a plasma, which reaches a few tenths of a degree under conditions of its heating by a high-power radio

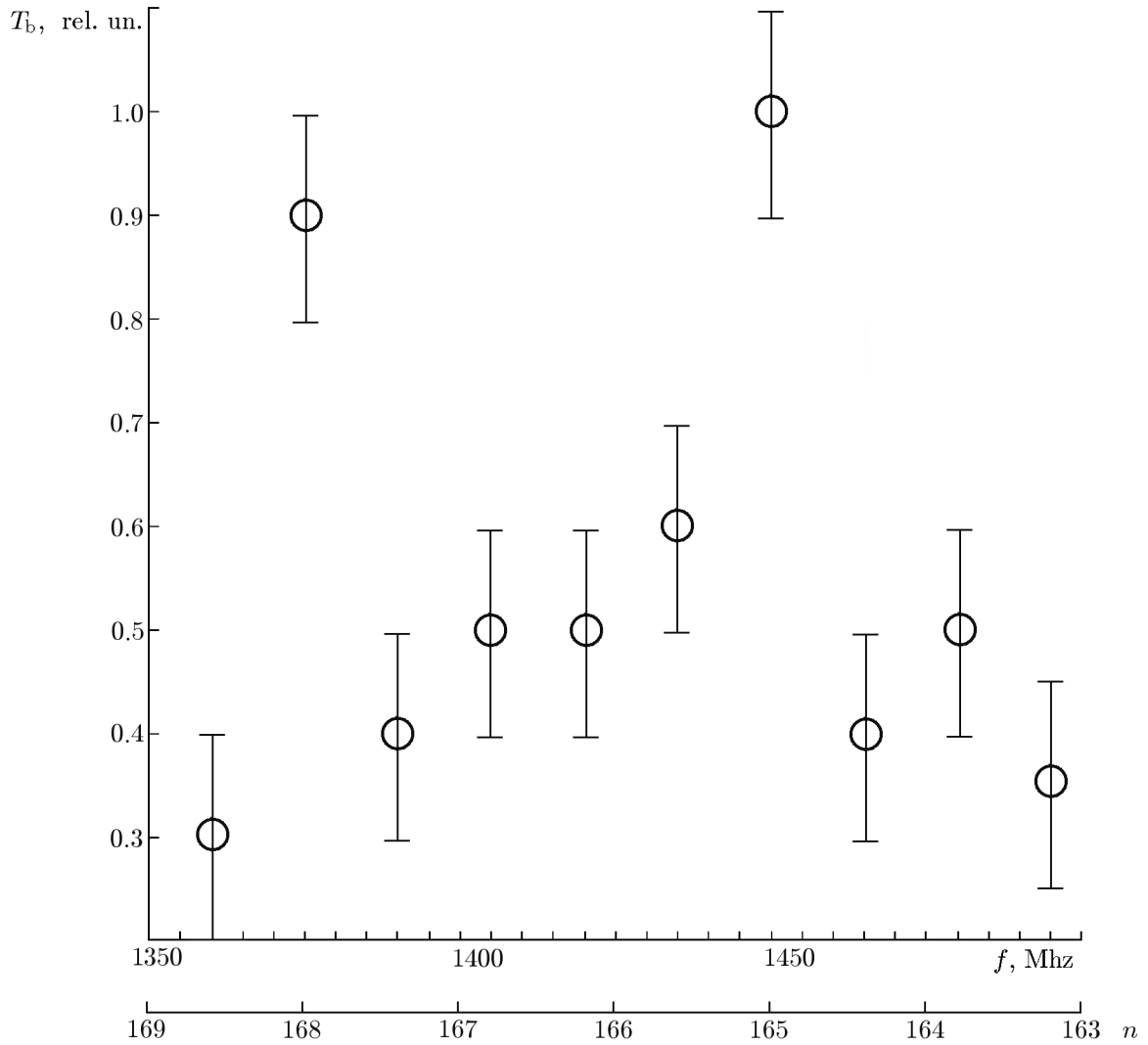


Fig. 4. Normalized spectrum of the atmospheric radiation intensity on April 2, 2015 in the frequency range 1350–1500 MHz with a 15-MHz resolution.

wave at the detection frequency 600 MHz.

Figure 4 shows the normalized spectrum of the atmospheric radiation intensity in the frequency range 1350–1500 MHz with a resolution of 15 MHz, which was obtained on April 2, 2015 when the ionosphere was affected by high-power radio waves from the Sura facility at the pump-wave frequency $f_{PW} = 6720$ kHz. The spectrum clearly distinguishes between two spectral maxima coinciding with the frequencies of transitions between Rydberg states $m = 169 \rightarrow n = 168$ with $\nu_n = 1375.35$ MHz and $m = 166 \rightarrow n = 165$ with $\nu_n = 1451.5$ MHz. Note that 5 Rydberg lines are located in the studied frequency range. The absence of pronounced spectral features for the other three lines can be explained by the inexact coincidence of the frequency of the spectral line with the frequency of the spectrum analyzer channel.

4. CONCLUSIONS

A new channel of impact on a neutral atmosphere through the excitation of Rydberg states of neutral atoms and molecules during ionosphere modification by high-power radio waves and the generation of microwave radiation has been detected. Characteristics of the microwave radiation of the upper atmosphere due to the emission of highly excited Rydberg atoms and molecules with principal quantum numbers $n = 163$ –169 and $n = 225$ (decimeter wavelength range) have been determined. The radiation intensity amounted

to a value corresponding to 10–45 K, and it was higher in the late evening and nighttime hours when interaction between a high-power radio wave and the plasma of the ionospheric F_2 region was most effective, leading to acceleration of electrons to suprathermal energies [14–16] and to intense precipitation of energetic electrons from the Earth’s radiation belt [17]. The results of the studies prove the effectiveness of the mechanism of the formation of highly excited Rydberg states of atoms and molecules in the ionosphere modified by high-power HF radio waves and indicate the existence of a Rydberg channel for generating microwave radiation at ionospheric altitudes, the intensity of which is comparable with the radio emission generated during solar flares. It is important to emphasize that this radiation, freely propagating down to the Earth’s surface, affects the processes occurring in the mesosphere, thermosphere, and troposphere.

The studies were supported by the Ministry of Education and Science (project No. 3.1844.2017/4.6).

REFERENCES

1. E. A. Benediktov, Yu. S. Korobkov, N. A. Mityakov, et al., *Izv. Vyssh. Uchebn. Zaved., Radiophys.*, **3**, No. 6, 957 (1960).
2. V. S. Troitskii, L. N. Bondar’, and A. M. Starodubtsev, *Dokl. Akad. Nauk SSSR*, **212**, No. 3, 719 (1973).
3. V. S. Troitskii, A. M. Starodubtsev, L. N. Bondar’, et al., *Radiophys. Quantum Electron.*, **16**, No. 3, 239 (1973).
4. L. N. Bondar’, K. M. Sterzhneva, and V. S. Troitskii, *Astron. Vestnik*, **9**, No. 4, 210 (1975).
5. S. I. Musatenko, *Geomagn. Aéron.*, **20**, No. 5, 884 (1980).
6. S. V. Avakyan, A. E. Serova, and N. A. Voronin, *Geomagn. Aéron.*, **37**, No. 3, 99 (1977).
7. R. L. Sorochenko and M. A. Gordon, *Recombination Radio Lines. Physics and Astronomy*, Fizmatlit, Moscow (2003).
8. S. M. Grach, V. M. Fridman, L. M. Lifshits, et al., *Ann. Geophysicae*, **20**, No. 10, 1687 (2002).
9. M. G. Golubkov, D. Sc. Thesis “Collective Rydberg states in the Earth’s upper atmosphere” [in Russian], Federal Research Center of Chemical Physics of the Russian Academy of Sciences, Moscow (2015).
10. V. L. Krauklis, G. A. Nikol’sky, M. M. Safronova, and E. O. Shults, *Oceanic Optics*, **3**, No. 3, 20 (1990).
11. S. V. Avakyan and N. A. Voronin, *Issled. Zemli Kosm.*, No. 2, 28 (2007).
12. S. V. Avakyan, A. V. Troitskii, and S. A. Chernous, in: *Proc. 17th All-Union Sci. Techn. Conf. “Topical Problems of Safety and Protection,” St. Petersburg, April 2–3, 2014*, p. 116.
13. A. V. Gurevich, *Nonlinear Phenomena in the Ionosphere*, Springer, New York (1978).
14. A. V. Gurevich, *Phys. Usp.*, **50**, No. 11, 1091 (2007).
15. A. V. Streltsov, J.-J. Berthelier, A. A. Chernyshov, et al., *Space Sci. Rev.*, **214**, No. 8, 118 (2018).
16. V. L. Frolov, *Artificial Turbulence of the Midlatitude Ionosphere* [in Russian], NNSU Press, Nizhny Novgorod (2017).
17. V. L. Frolov, A. D. Akchurin, I. A. Bolotin, et al., *Radiophys. Quantum Electron.*, **62**, No. 9, 571 (2020).